INL/JOU-20-57814-Revision-0

XRD and SEM/EDS characterization of two quaternary fuel alloys (U-2.5Mo-2.5Ti-5.0Zr and U-1.5Mo-1.5Ti-7.0Zr) for fast reactors

December 2020

Weiqian Zhuo, Jianbang Ge, Michael T Benson, Yi Xie, Robert D Mariani, Jinsuo Zhang

Changing the World's Energy Future

Idaho National Laboratory

INL is a U.S. Department of Energy National Laboratory operated by Battelle Energy Alliance, LLC

INL/JOU-20-57814-Revision-0

XRD and SEM/EDS characterization of two quaternary fuel alloys (U-2.5Mo-2.5Ti-5.0Zr and U-1.5Mo-1.5Ti-7.0Zr) for fast reactors

Weiqian Zhuo, Jianbang Ge, Michael T Benson, Yi Xie, Robert D Mariani, Jinsuo Zhang

December 2020

Idaho National Laboratory
Idaho Falls, Idaho 83415

http://www.inl.gov

Prepared for the
U.S. Department of Energy
Under DOE Idaho Operations Office
Contract DE-AC07-05ID14517

XRD and SEM/EDS characterization of two quaternary fuel alloys (U-2.5Mo-2.5Ti-5.0Zr and U-1.5Mo-1.5Ti-7.0Zr in wt. %) for fast reactors

Weiqian Zhuo[a], Yi Xie[b], Michael T. Benson[c], Jianbang Ge[a], Robert D. Mariani[c], Jinsuo Zhang[a,*]

[a] Nuclear Engineering Program, Department of Mechanical Engineering,
Virginia Tech, Blacksburg, Virginia 24061, USA
[b] School of Nuclear Engineering, Purdue University, West Lafayette, IN 47906, USA
[c] Idaho National Laboratory, P.O. Box 1625, Idaho Falls, ID 83415, USA
*Corresponding author, Email: zjinsuo5@vt.edu

Abstract

The current study focuses on characterization of two potential fuel alloys for sodium-cooled fast reactors: U-2.5Mo-2.5Ti-5.0Zr (U-MT5Z) and U-1.5Mo-1.5Ti-7.0Zr (U-MT7Z) in wt. %. As-cast alloys and annealed (600 ^{o}C, 500 hours) alloys are studied by X-ray powder diffraction (XRD) for their bulk structures, and scanning electron microscopy / energy dispersive X-Ray spectroscopy (SEM/EDS) for their microstructures and phase constituents. For as-cast alloys, the XRD results show that U-MT5Z mainly contains γ , while U-MT7Z alloy contains α . In both alloys, there are three phases indicated by EDS, a U-rich matrix, secondary phase, and Zr-rich phase. The elemental compositions varied in different phases and in different alloys. After annealing, both alloys exhibit the structures of α-U and U_2Ti according to XRD. The EDS results suggest there are five phases found in both alloys.

Keywords – Fast reactor, metallic fuel, microstructure, grain boundaries, SEM/EDS, XRD;

1. Introduction

The sodium-cooled fast reactor (SFR) was developed over six decades ago. Development eventually led to the use of U-Zr fuel alloys, which have a higher solidus temperature than pure U metal, being one of the most common driver fuels for an SFR. Successful implementation of U-Zr has been achieved in the Experimental Breeder Reactor-II (EBR-II) and Fast Flux Test Facility (FFTF) in the U.S. However, it has a drawback of constituent redistribution due to multiple phases at reactor operation temperatures [1]. The U-Mo alloy is another possible candidate for SFRs [2, 3, 4]. Relevant irradiation tests showed U-Mo alloys had the benefits of isotropic growth [2] and no constituent redistribution [4], but more fuel cladding chemical interactions (FCCIs) were observed with U-10Mo as compared to U-10Zr [4]. The FCCIs are caused by the chemical inter-diffusion of the fuel and cladding constituents, and they will lead to a multi-phase region that places both the fuel and cladding at risk [5]. Available data showed that a significant amount of FCCI had occurred in U-10Mo fuels, resulting in cladding thinning [4]. In contrast, little FCCI was observed in the U-10Zr fuel under similar irradiation condition [4].

Recently, a new quaternary alloy with the constituents U, Mo, Zr, and Ti was proposed, and some relevant investigations were initiated [1, 6, 7]. By alloying Mo, Zr, and Ti with U, the expectation is to decrease the γ phase onset temperature (due to Mo) and increase the solidus/liquidus temperatures (due to Zr and Ti) for uranium [1]. The γ phase onset temperature refers to the temperature above which the γ phase starts to form (for example, it is 776 °C for pure uranium [8, 9], 555 °C for U-10Mo [8], and around 690 °C for U-10Zr [9, 10]). If the γ phase onset temperature is decreased, the amount of γ phase will increase in a typical fuel temperature range (around 450°C to 700°C [11]). The γ phase is a favorable phase because of its body-centered-cubic (bcc) structure. With the bcc structure, predictable isotropic swelling behavior can be expected [12, 13]. In addition, available studies show that the Mo-Ti-Zr system has a large bcc region under high temperatures [6, 14, 15]. Therefore, exploratory research on quaternary U-Mo-Ti-Zr (or U-MTZ) alloys has been initiated. Some preliminary investigations have been performed on the 90.0U-5.0Mo-4.3Ti-0.7Zr (wt. %) alloy [4, 16, 17, 18]. Constituent redistribution was not observed in this alloy, but there was significant fuel-cladding chemical interaction (FCCI) during irradiation, primarily due to the low Zr content and high Mo content [16]. Based on these results, it is necessary to adjust the ratio of Mo-Ti-Zr in the U-MTZ alloy. In order to reduce FCCI, the concentration of Mo will need to decrease, and the Zr concentration will need to increase. This is the rational for the chosen alloys in this study. The Mo content has been decreased and the Zr content has been increased, with the goal of retaining the beneficial aspects of each alloying element while reducing FCCI due to Mo. The targeted alloys are listed in Table 1. The goal of this investigation is not the optimization of the U-MTZ composition, but an initial characterization of two lower-Mo, higher-Zr compositions.

Table 1. Targeted alloy compositions.

Alloy	wt. %	at. %
U-MT5Z	90.0U-2.5Mo-2.5Ti-5.0Zr	74.0U-5.1Mo-10.2Ti-10.7Zr
U-MT7Z	90.0U-1.5Mo-1.5Ti-7.0Zr	75.4U-3.1Mo-6.2Ti-15.3Zr

In both alloys, the content of U is 90 wt. %, and total content of MTZ is 10 wt. %. For the MTZ fraction, the Zr content is higher (5 wt. % or 7 wt. %), and the contents of Mo and Ti are equal in weight percent (2.5 wt. % or 1.5 wt. %). For simplicity, the weight percent of Zr (i.e., the number before Z) will be used to differentiate these two alloys, so the alloys names are U-MT5Z or U-MT7Z.

Before testing the alloys in a reactor, the first step is to gain basic information of the phase and the microstructure through out-of-pile investigation. This study is focusing on the as-cast samples and the samples annealed at 600 °C for 500 hours. This temperature was selected because it is in the typical fuel temperatures range. To allow the transformation to take place, the annealing time varied from tens to hundreds of hours, according to the related studies [19, 20, 21]. Based on this, 500 hours was chosen to allow sufficient time for the phase formation in the alloys. There are four samples (i.e., as-cast and annealed U-MT5Z, as-cast and annealed U-MT7Z) characterized in this study. Each sample was characterized by X-ray diffractometry (XRD) for bulk phase identification, and scanning electron microscopy/energy dispersive X-ray spectrometry (SEM/EDS) for microstructure and phase constituents.

2. Materials and Experiments

All materials except U were obtained from Alfa Aesar and used as received. All casting operations were carried out in an arc-melter within an argon atmosphere glovebox (oxygen < 10 ppm) with high purity argon as a cover gas. The appropriate amount of U, Mo, Ti, and Zr were arc-melted together in two steps. The first step was melting Mo, Ti, and Zr together, followed by addition of U. After each step, the cast button was flipped and re-melted three times to ensure homogeneity. The resulting buttons of U-Mo-Ti-Zr were cast into 5 mm diameter pins using a drop casting technique. An approximately 2 mm thick sample pellet was cut from each pin and used for the study. The alloys were cast at Idaho National Laboratory but the tests and characterization were performed at Virginia Tech. The annealing tests were performed in a furnace inside a glove box filled with high purity argon (99.999%). The oxygen and moisture were maintained at ppm level (oxygen < 10 ppm, moisture < 1 ppm) during annealing. The samples were heated at 600°C for 500 hours. After the heat treatment, the samples were taken out of the furnace and placed in a Si-based quenching oil for 1 min to preserve the high-temperature phases.

Before performing XRD, the samples were ground using SiC sandpapers (with grit size 240, 400, 800) to remove the oxide layer and obtain a flat surface. A PANalytical Empyrean XRD equipped with a copper source was employed for the analysis. In each XRD scan, the step size was 0.007162 °/step, and the scan rate was 1°/min.

Before performing SEM/EDS, the samples were ground using SiC sandpapers (with grit size 600, 800, 1000, 1200) followed by polishing using polycrystalline diamond suspensions (1 μm, 0.25 μm, 0.05 μm) in air. To reveal the grain of as-cast alloys, chemical etching was applied on the sample surface after polishing. Concentrated HNO_3 (70% w/w) was used as the etchant. The etching was performed in a stepwise manner. If the etching time was too short, the grains were not revealed, and if the etching time was too long, the etchant destroyed the surface morphology. To etch the surface, a drop of HNO_3 was applied on the surface and held for 1 to 2 minutes,

followed by rinsing the sample in deionized water. The surface was then examined using SEM. This was repeated until a sufficient etching time (10-20 minutes in total) was reached. Various methods have been reported for etching uranium-base alloys. Chemical etching or electrolytic etching can be used, although an acid solution is typically chosen as the etchant [22, 23]. Etching with HNO_3 was adopted in the current study, providing a straightforward method to etch the U-MTZ alloys effectively. The SEM was performed on the FEI Quanta 600 FEG equipped with a Bruker energy dispersive spectrometer. The energy line was calibrated with L-α and K-α from a high purity Cu disk. The SEM was operated at an accelerating voltage of 20 kV with spot size 5. EDS data was collected using the ESPRIT 1.9 software. Deconvolution and quantification methods were serials fit and P/B ZAF (standardless). When quantifying the chemical composition of the phase, the alloy constituents, i.e., U, Mo, Ti, Zr were selected, while light elements such as oxygen and carbon were excluded. In the analysis, the spectra were collected up to 10 keV. The EDS spatial resolution was 1-1.5 μm. The error from the EDS measurement is less than 1 percent.

3. Results

The bulk composition of each alloy was measured via EDS. The measurements were performed on three random rectangular areas (about 0.5mm×0.5mm) on the surface, and the average value for each element is reported in Table 2. According to the data, the measured composition is close to the targeted composition, and the overall composition is stable upon annealing.

Table 2. Average composition* of the bulk material (wt. %).

Alloy		U	Mo	Ti	Zr
U-MT5Z	As-cast	90	2	3	5
	Annealed	89	2	3	6
U-MT7Z	As-cast	90	1	2	7
	Annealed	90	1	2	7

*Average composition as measured using SEM-EDS covering three random rectangular areas (about 0.5mm×0.5mm).

3.1 U-MT5Z

In this section, data for the as-cast alloy will be presented first, followed by data for the annealed alloy. This format will also be used when presenting the data for the U-MT7Z alloy in Section 3.2.

3.1.1 As-cast U-MT5Z alloy

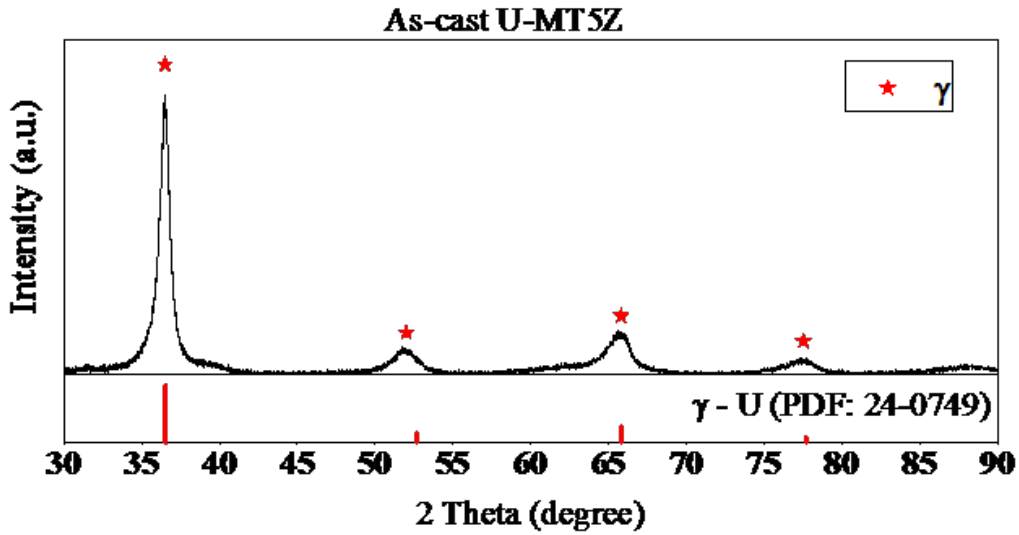

Figure 1. XRD result for the as-cast U-MT5Z alloy.

The XRD result for the as-cast U-MT5Z alloy is shown in Figure 1, with γ phase being observed. The microstructure of the sample was characterized by SEM/EDS. The representative backscattered electron (BSE) images are shown in Figure 2, with the surface morphologies before and after etching at the same area. For the surface before etching (Figure 2a and b), there are three contrast areas found, i.e. bright, grey and black. To quantify the compositions, EDS point scans were performed, and the corresponding data is listed in Table 3. The bright region mainly contains U, and a portion of Mo, Ti, and Zr, thus it is suggested to be a U-rich phase. The grey region is suggested to be a secondary phase, as it contains more Ti and Zr than that of the U-rich phase, the ratio of U to (Ti, Zr, Mo) is closed to 2:1. In the matrix and the secondary phase, the content of Mo is around 3 to 4 at%, and the ratio of Ti and Zr is close to 1:1. The black precipitates are Zr-rich phases with a small amount of U and Ti. The Zr precipitates are commonly observed in U-Zr base alloys [24, 25, 26, 27, 28], possibly formed by impurity such as C, O, N during the fabrication [27]. The surface morphologies after etching are shown in Figure 2b and d. Etching makes the secondary phase (relief-like) clearer, and also revealing the grain boundaries. The EDS point data show that the compositions of the phases are close to that before etching.

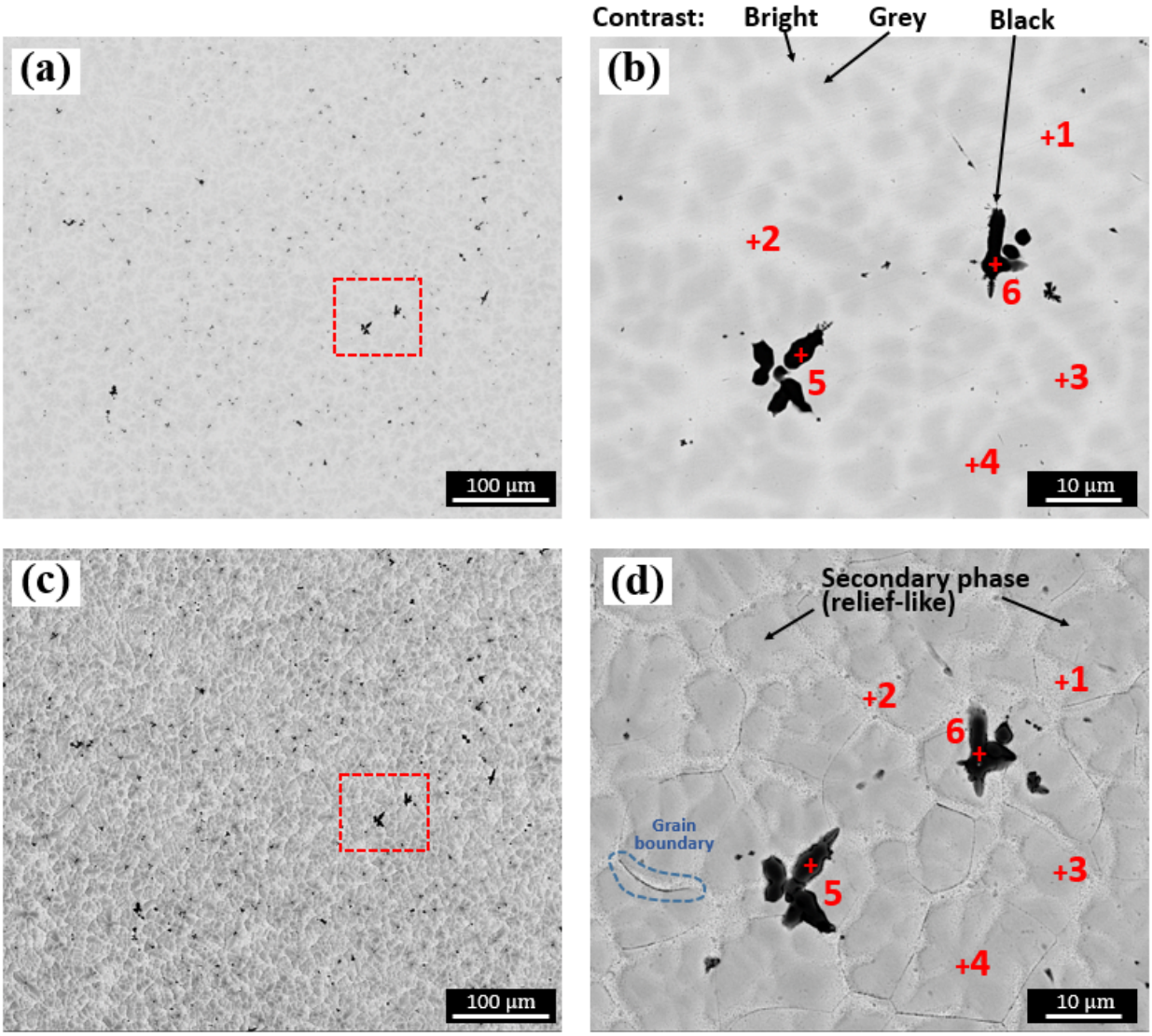

Figure 2. Back-scattered electron (BSE) images for U-MT5Z, (a) and (b) are before etching, while (c) and (d) are after etching. (b) is the higher magnification image for the region indicated by the red rectangle in (a), and (d) is the higher magnification image for the region indicated by the red rectangle in (c). The corresponding EDS data are listed in Table 3.

Table 3. EDS analysis for data points shown in Figure 2 (at. %).

	U	Mo	Ti	Zr	Phase*	Contrast
Figure 2b						
1	82	4	7	7	U-rich	Bright
2	84	3	6	7	U-rich	Bright
3	69	3	13	15	Secondary phase	Grey
4	68	3	14	15	Secondary phase	Grey
5	2	1	6	91	Zr-rich	Black
6	3	0	6	90	Zr-rich	Black
Figure 2d						

1	80	3	9	8	U-rich (matrix)	Bright
2	84	2	7	7	U-rich (matrix)	Bright
3	70	5	11	14	Secondary phase	Grey
4	69	3	14	14	Secondary phase	Grey
5	1	0	7	92	Zr-rich	Black
6	2	0	7	91	Zr-rich	Black

* Suggested phase based on EDS analysis

3.1.2 Annealed U-MT5Z alloy

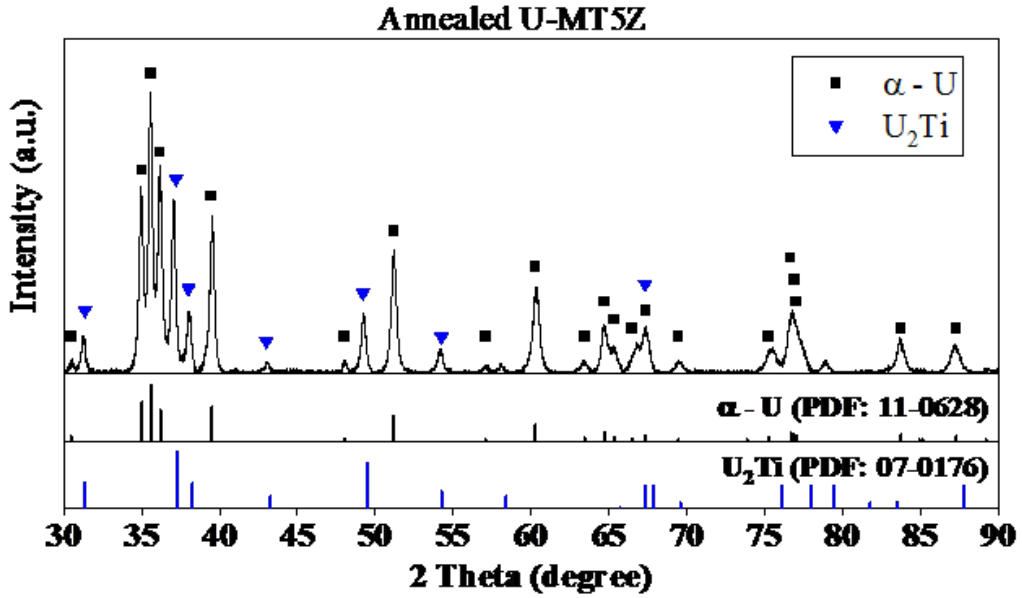

Figure 3. XRD result for the annealed U-MT5Z alloy.

The XRD result for the annealed U-MT5Z alloy is shown in Figure 3, with α-U and U_2Ti identified. The SEM/EDS characterization revealed a complex phase morphology, with representative images shown in Figure 4. According to the analysis, there are five phases observed:

1. α-U phase. The bright region contains pure uranium, according to EDS points 1, 2 and 3 in Figure 4b. The XRD data (Figure 3) indicate that α-U is found on the annealed alloy. For these reasons, the bright region is identified as α-U.
2. U_2Ti, the light grey region indicated by EDS points 4, 5, and 6 in Figure 4b. According to the EDS data (Table 4), this region primarily contains U and Ti with small amounts of Mo and Zr. The ratio of U and Ti is close to 2:1. In the XRD spectrum (Figure 3), the U_2Ti pattern is present. Thus, it is believed this phase is U_2Ti (hexagonal, space group P6/mmm). Mo and Zr were detected probably because there are small amounts of Mo and Zr dissolved in the phase or due to the interaction volume of the electron beam.
3. U-Zr compound, the dark grey region indicated by EDS points 7 and 8 in Figure 4b. It mainly contains U and Zr with some Mo and Ti. The reasons for the presence of Mo and Ti are similar to that in U_2Ti, i.e., maybe there are small amounts of Mo and Zr dissolved

in the phase or due to the interaction volume of the beam.

4. Zr-rich phase, the black precipitate indicated by EDS point 11 in Figure 4b. A high Zr content was detected according to the EDS point data. By the elemental map in Figure 4f, Zr is enriched in that precipitate. Similarly, the black precipitates, EDS points 1 and 2 in Figure 4a are Zr-rich phases as well.
5. An unidentified phase, the black precipitate indicated by EDS points 9 and 10 in Figure 4b. The size of the phase is too small, so the compositional data may not be accurate due to the interaction volume of the electron beam. According to the EDS maps (Figure 4d), Mo is found to be enriched in those precipitates.

Comparisons of the microstructures between as-cast and annealed samples indicate that the phases are changed after annealing. There are three phases in the as-cast alloy, but five phases are observed in the annealed alloy, as summarized in Table 5. The Zr-rich phase appears to be stable, because the compositions between the as-cast (points 5 and 6 in Figure 2b or c) and annealed samples (points 1 and 2 in Figure 4a) are very similar compositionally. The matrix and the secondary phase changed significantly during the annealing. These two regions are now α-U, U_2Ti, U-Zr compound, and an unidentified phase after annealing.

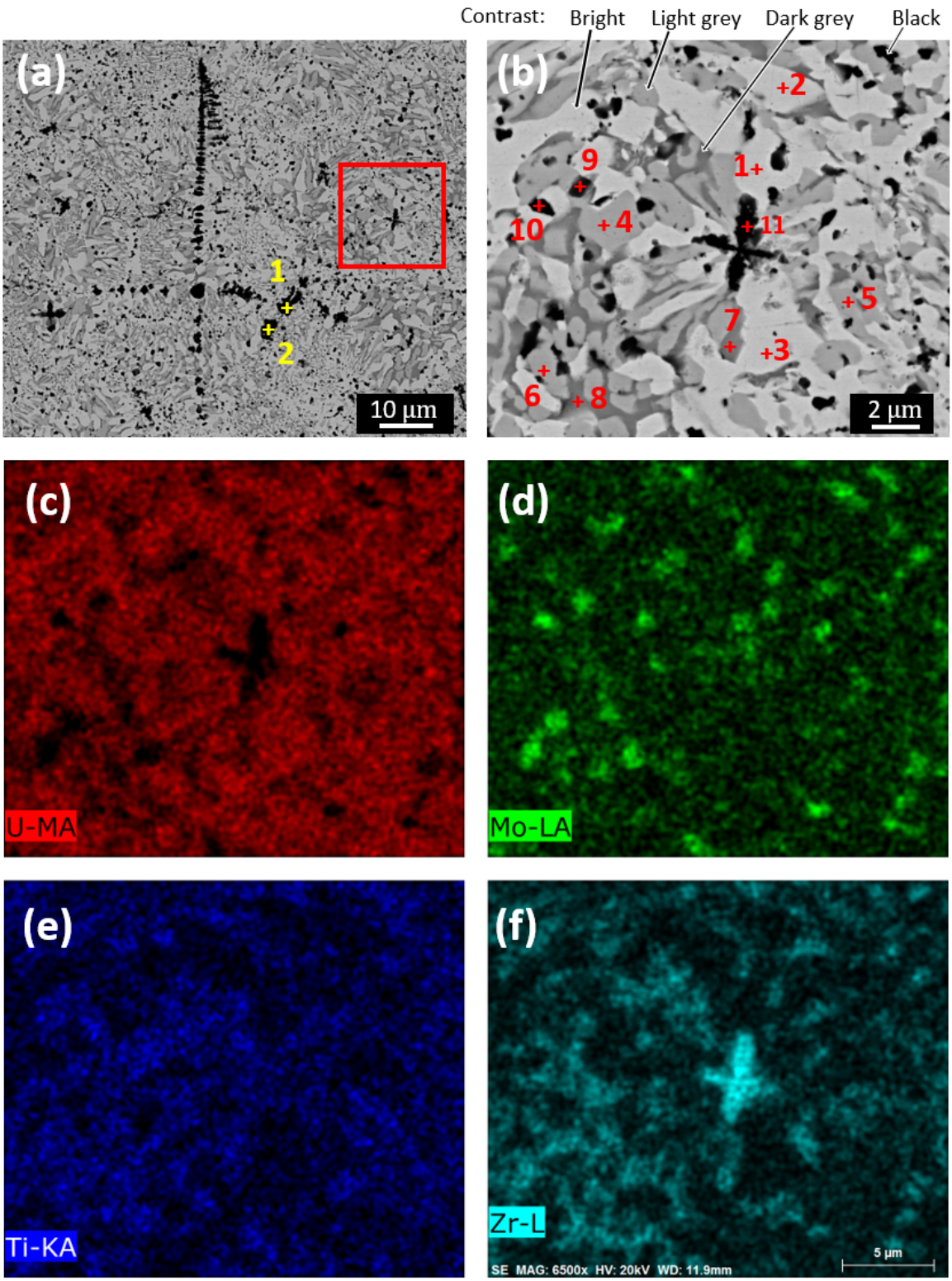

Figure 4. BSE images for annealed U-MT5Z, (a) at 3000× magnification and (b) is the magnified region indicated by the red square in (a), (c) to (f) are EDS elemental maps for (b). The corresponding EDS data are listed in Table 4.

Table 4. EDS analysis for data points shown in Figure 4 (at. %)

	U	Mo	Ti	Zr	Phase	Contrast
Figure 4a						
1	2	1	9	88	Zr-rich	Black
2	1	0	9	89	Zr-rich	Black
Figure 4b						
1	99	0	0	1	α-U	Bright
2	100	0	0	0	α-U	Bright
3	100	0	0	0	α-U	Bright
4	66	2	28	4	U_2Ti	Light grey
5	64	3	27	6	U_2Ti	Light grey
6	65	3	28	4	U_2Ti	Light grey
7	54	4	5	37	U-Zr compound	Dark grey
8	44	6	8	42	U-Zr compound	Dark grey
9	27	31	17	25	Unidentified	Black
10	23	37	11	29	Unidentified	Black
11	17	9	11	63	Zr-rich	Black

Table 5. The phases observed in U-MT5Z alloy

Sample	Phases observed
As-cast	• U-rich • A secondary phase • Zr-rich
Annealed	• α-U • U_2Ti • U-Zr compound • Zr-rich • An unidentified phase

3.2 U-MT7Z

3.2.1 As-cast U-MT7Z alloy

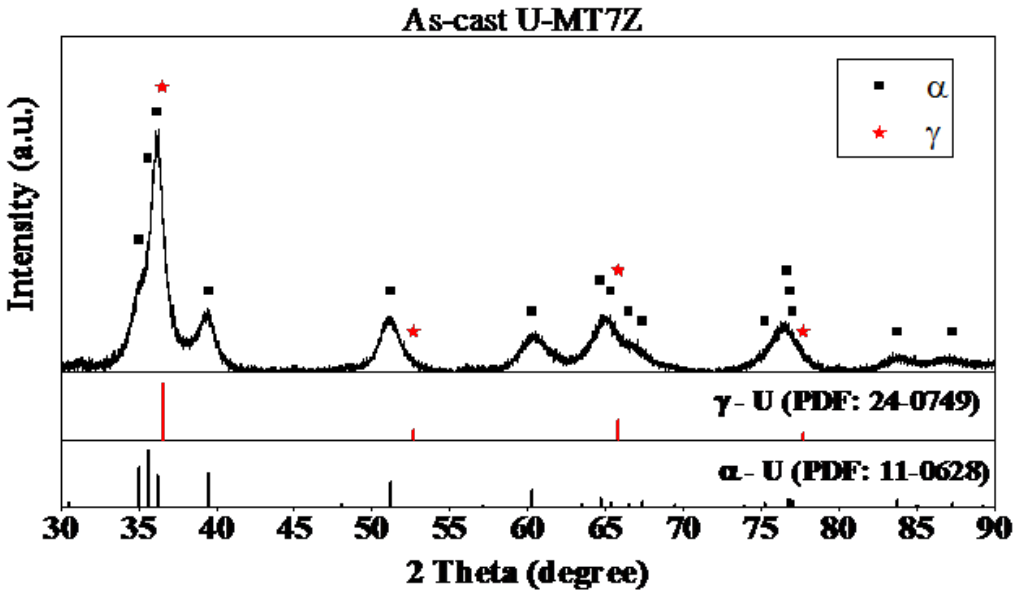

Figure 5. XRD result for the as-cast U-MT7Z alloy

The XRD result for the as-cast U-MT7Z alloy is shown in Figure 5. The as-cast sample mainly contains α-U, but it is very difficult to determine if there is γ present or not due to peak overlap. This is significantly different from as-cast U-MT5Z, which contains γ phase. The difference between these two alloys is the composition change in Mo, Ti, Zr. However, Mo is a strong γ stabilizer [6, 29], and the U-MT5Z alloy has a higher concentration of Mo, which stabilizes the γ phase during fabrication.

Figure 6 shows the BSE images of as-cast U-MT7Z before and after etching. The U-rich (bright), a secondary phase (grey) and Zr-rich phase (black) are the three phases found. Again, the etching makes the secondary phase more apparent. The EDS point data are listed in Table 6, showing the content in these phases differ from that in the U-MT5Z alloy. The change in composition can be attributed to the change in MTZ composition. There is less Zr, and more Mo and Ti, in MT5Z than there is in MT7Z.

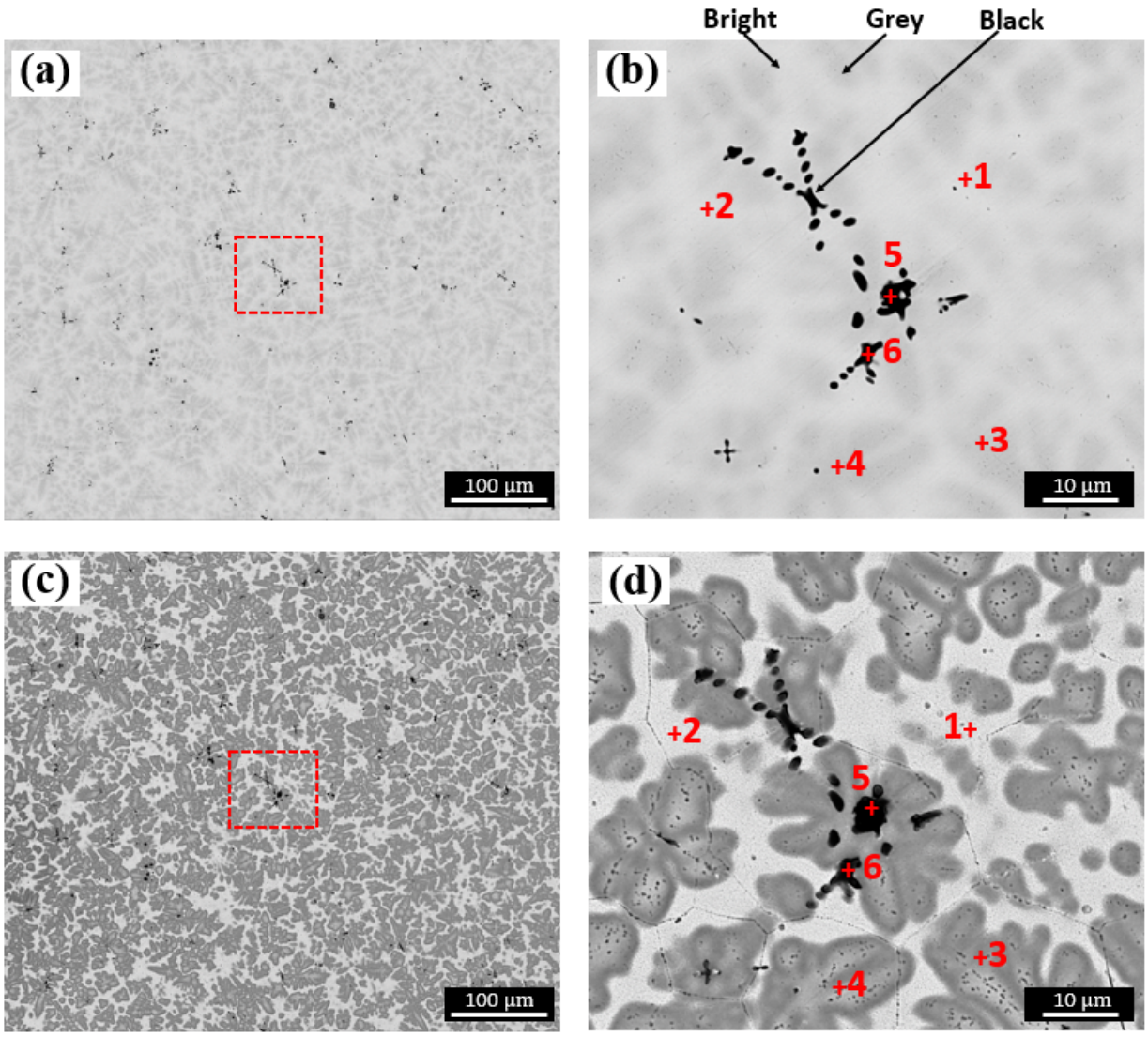

Figure 6. BSE images for U-MT7Z, (a) and (b) are the morphologies before etching, (c) and (d) are the morphologies after etching. (b) is the higher magnification image for the region indicated by the red rectangle in (a), and (d) is the higher magnification image for the region indicated by the red rectangle in (c). The corresponding EDS data are listed in Table 6.

Table 6. EDS analysis for data points shown in Figure 6 (at. %)

	U	Mo	Ti	Zr	Phase*	Contrast
Figure 6b						
1	89	2	3	6	U-rich	Bright
2	85	2	4	9	U-rich	Bright
3	67	3	8	22	Secondary phase	Grey
4	61	3	9	27	Secondary phase	Grey
5	9	0	7	84	Zr-rich	Black
6	24	1	5	70	Zr-rich	Black
Figure 6d						
1	86	1	3	10	U-rich	Bright

2	87	2	3	8	U-rich	Bright
3	68	3	7	24	Secondary phase	Grey
4	65	2	8	25	Secondary phase	Grey
5	9	2	4	85	Zr-rich	Black
6	20	1	7	72	Zr-rich	Black

* Suggested phase based on EDS analysis

3.2.2 Annealed U-MT7Z alloy

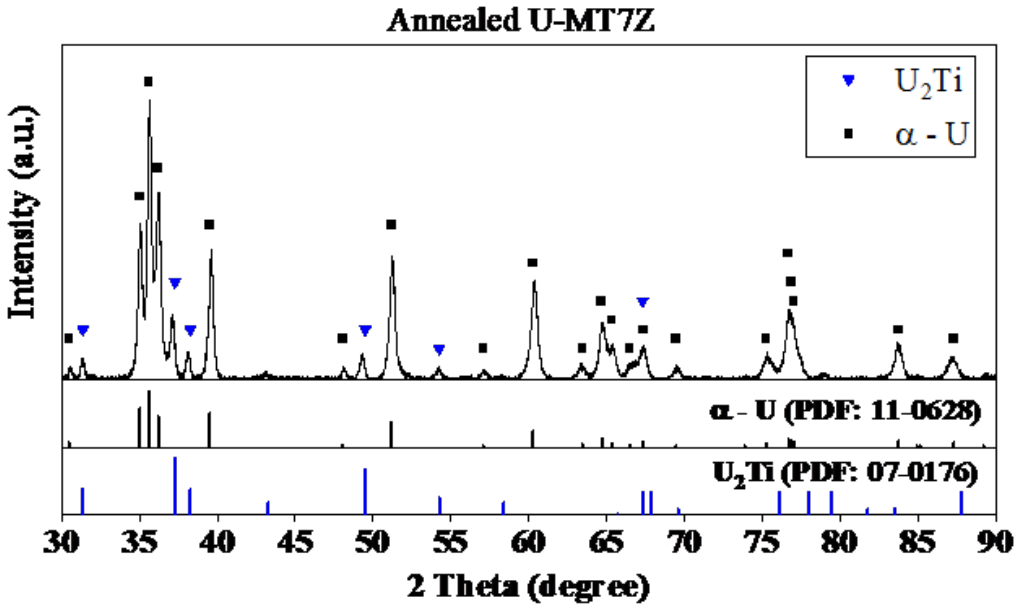

Figure 7. XRD result for the annealed U-MT7Z alloy

The XRD result for the annealed U-MT7Z alloy is shown in Figure 7. The composition is primarily α-U and U_2Ti, similar to that in the annealed U-MT5Z alloy. The representative images from SEM/EDS characterization are shown in Figure 8. The observation is similar to that in U-MT5Z, but the grain boundaries have been revealed associated with the multi-phase formation. α-U, U_2Ti, U-Zr compound with small amounts of Mo and Zr, and Zr-rich phases are analogous to those in the annealed U-MT5Z alloy. EDS analysis for the points shown in Figure 7 is listed in Table 7. Some black spots with a size smaller than 1 μm are found at the grain boundaries (for example, the spots associated with points 7 and 8 in Figure 8b). The phase of these precipitates cannot be identified due to the limitation of SEM/EDS resolution, though. The phases observed in U-MT7Z are summarized in Table 8.

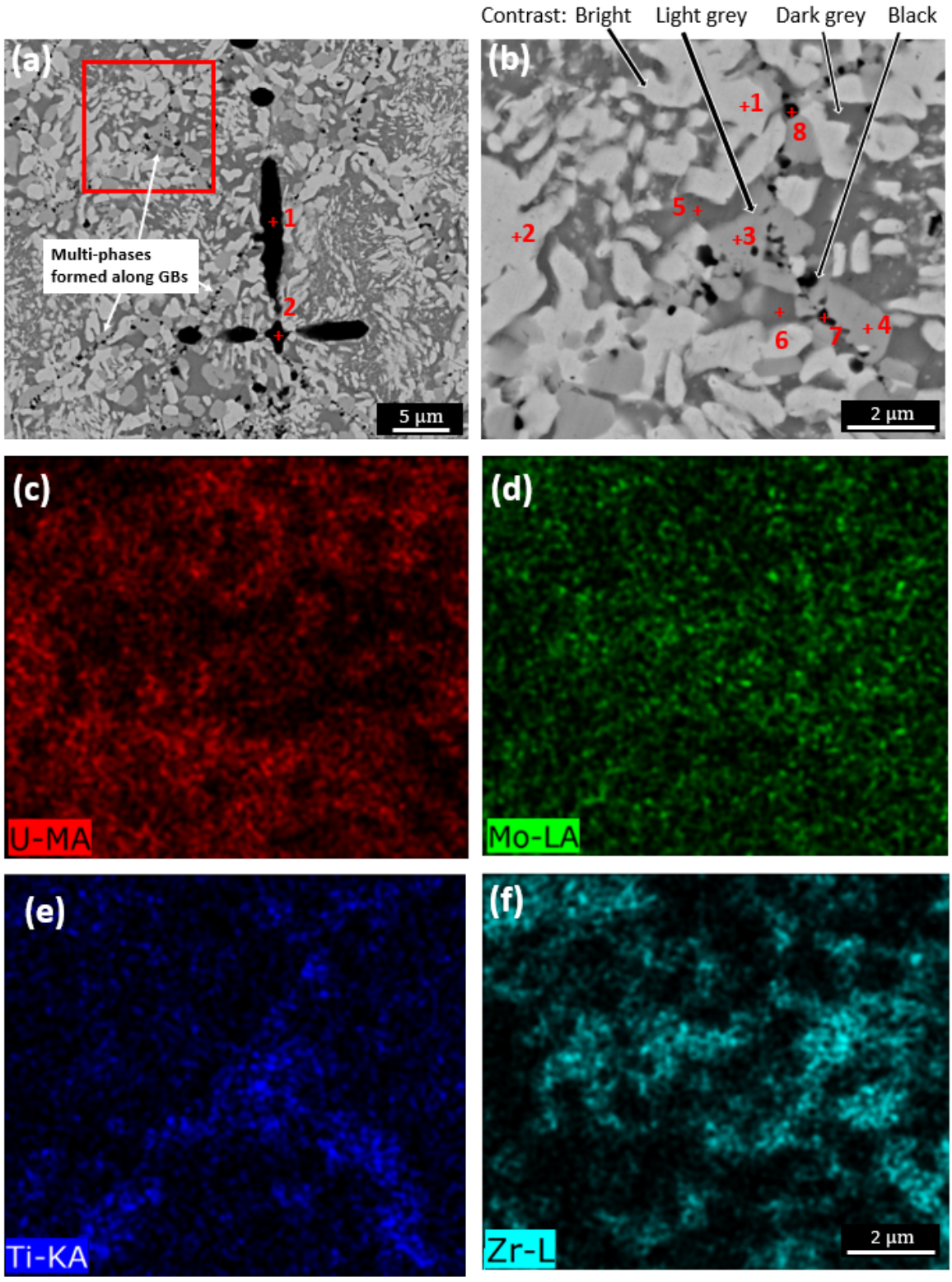

Figure 8. BSE images for annealed U-MT7Z: (a) at 7000× magnification; (b) is the magnified region indicated by the red square in (a). (c) to (f) are EDS elemental maps for (b). The corresponding EDS data are listed in Table 7.

Table 7. EDS analysis for data points shown in Figure 8 (at. %).

	U	Mo	Ti	Zr	Phase	Contrast
Figure 8a						
1	4	0	5	91	Zr-rich	Black
2	4	0	5	91	Zr-rich	Black
Figure 8b						
1	98	0	1	1	α-U	Bright
2	98	0	0	2	α-U	Bright
3	65	2	28	5	U_2Ti	Light grey
4	65	3	27	7	U_2Ti	Light grey
5	44	6	7	43	U-Zr compound	Dark grey
6	45	6	9	40	U-Zr compound	Dark grey
7	47	8	15	30	Unidentified	Black
8	47	10	6	37	Unidentified	Black

Table 8. The phases observed in U-MT7Z alloy

Sample	Phases observed
As-cast	• U-rich • A secondary phase • Zr-rich
Annealed	• α-U • U_2Ti • U-Zr compound • Zr-rich • An unidentified phase

3.3 Discussion on the grain size

In a metallic fuel, the fission gas bubbles nucleate at the grain boundaries [30], and the grain boundaries are the major path of fission gas release [31]. The fuel with smaller grain will lead to a higher fission gas release rate during irradiation [31]. Therefore, it is necessary to gain a better understanding of the grain morphologies in those alloys.

In as-cast U-MT5Z, the grain size decreases from the center region to the edge of the sample pellet. Three typical grain structures in U-MT5Z pellet (5 mm radius) are shown in Figure 9. In the center region (Figure 9a), the grain size is as large as 20~30 μm, and the grain boundary could be surrounded by the secondary phase or passing through it (Figure *2*d). In the middle region (Figure 9b), the grain size is around 10 to 20 μm, and in edge region (Figure 9c), the grain size is around 10 μm, and the grain boundary is more likely to be surrounded by the secondary phase. It is known that the cooling rate affects the grain size and that faster cooling will generally result in a smaller grain size [32]. The fuel rod cooled down from the edge to the middle during drop-casting, so the edge was subjected to a faster cooling rate than the rod center, resulting in smaller grain size at the edge of the rod.

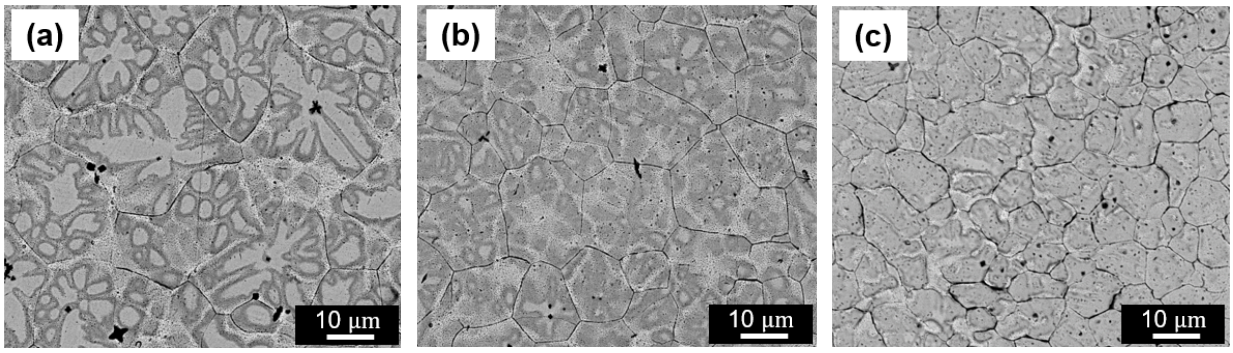

Figure 9. BSE images taken from (a) center region, (b) middle region, and (c) edge region showing the grain size in the as-cast U-MT5Z alloy.

In annealed U-MT5Z, the grains cannot be clearly identified, even with etching. An acid etchant produces a porous surface, not allowing the grain boundaries to be differentiated. Due to this, a comparison of the grain size between as-cast sample and annealed sample is not possible.

For as-cast U-MT7Z, the grain sizes are similar everywhere on the whole pellet. The trend observed in the U-MT5Z alloy (decreasing from center to edge) does not show up. A typical grain morphology for the as-cast alloy is shown in Figure 10a. The grain morphology of the annealed alloy is shown in Figure 10b. The grain size varies from several µm to about 30 µm in both samples, but the grain growth is observed after annealing.

The grain size of the as-cast U-10Zr is about 60 µm [33], but the data for the annealed U-10Zr is limited. The grain size for as-cast U-10Mo is in the range of 10 to 50 µm [34], while for annealed alloy the it is around 10 to 150 µm, depending on the annealing temperature and time [35, 36, 37]. The grain size observed in the U-MT5Z and U-MT7Z has the same order of that in U-10Mo.

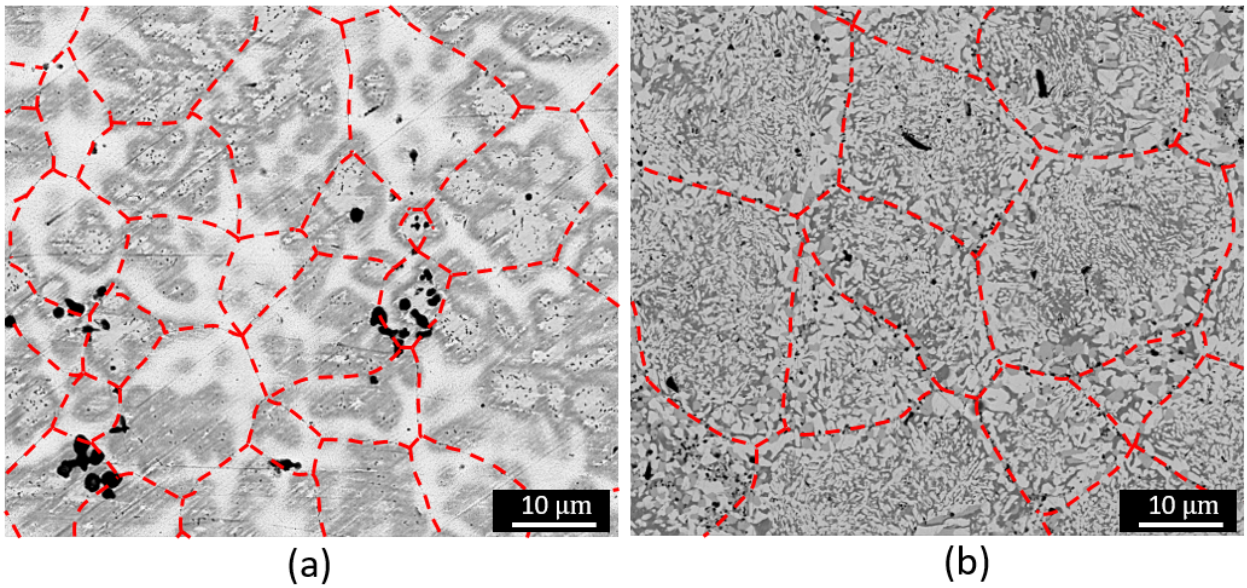

Figure *10*. Grains in (a) as-cast etched sample and (b) annealed sample of U-MT7Z alloy, artificial lines are drawn on the grain boundaries to enhance the readability.

4. Conclusion

In this work, two U-MTZ alloys (as-cast and annealing at 600 °C for 500h) are studied using XRD analysis for their bulk structures and SEM/EDS technique for their microstructures and phase compositions. For the as-cast alloys, the XRD results indicate that U-MT5Z is primarily γ-U, while U-MT7Z alloy is α-U. Under SEM, a secondary phase is observed in both alloys, but the atomic ratios of Ti to Zr are different. The approximate Ti to Zr ratio is 1:1 in U-MT5Z, while it is 1:3 in U-MT7Z. Upon annealing, the grain can be differentiated in U-MT7Z while it cannot in U-MT5Z. The present study also shows that 1.5 wt.% Mo is not enough to stabilize the gamma phase, while 2.5 wt.% Mo is enough. This is a positive because the results imply that not too much Mo is needed to stabilize gamma phase. It is beneficial for the fuel composition, given the FCCI issue with Mo. Less Mo is preferred when using Fe-base cladding.

Acknowledgement

This work was supported through the INL Laboratory Directed Research& Development (LDRD) Program under DOE Idaho Operations Office Contract DE-AC07-05ID14517. Accordingly, the U.S. Government retains and the publisher, by accepting the article for publication, acknowledges that the U.S. Government retains a nonexclusive, paid-up, irrevocable, worldwide license to publish or reproduce the published form of this manuscript or allow others to do so, for U.S. Government purposes. The advice and help by Nanoscale Characterization and Fabrication Laboratory at Virginia Tech is also highly appreciated.

Data availability

The processed data required to reproduce these findings are available by e-mail to the corresponding author: zjinsuo5@vt.edu

Declaration of competing interest

The authors declare that they have no known competing financial interests or personal relationships that could have appeared to influence the work reported in this paper.

Reference

[1] R.D. Mariani, D.L. Porter, S.L. Hayes, J.R. Kennedy, Metallic Fuels : The EBR-II legacy and recent advances, Procedia Chem. 7 (2012) 513–520. doi:10.1016/j.proche.2012.10.078.

[2] J.H. Kittel, B.R.T. Frost, J.P. Mustelier, K.Q. Bagley, G.C. Crittenden, J. Van Dievoet, History of fast reactor fuel development, J. Nucl. Mater. (1993). doi:10.1016/0022-3115(93)90193-3.

[3] A.E. Wright, S.L. Hayes, T.H. Bauer, H.J. Chichester, G.L. Hofman, J.R. Kennedy, T.K. Kim, Y.S. Kim, R.D. Mariani, W.D. Pointer, Development of advanced ultra-high burnup SFR metallic fuel concept- project overview, Trans. Am. Nucl. Soc. 106 (2012) 1102–1105.
[4] J.M. Harp, H.J.M. Chichester, L. Capriotti, Postirradiation examination results of several metallic fuel alloys and forms from low burnup AFC irradiations, J. Nucl. Mater. 509 (2018) 377–391. doi:10.1016/j.jnucmat.2018.07.003.
[5] C. Matthews, C. Unal, J. Galloway, D.D. Keiser, S.L. Hayes, Fuel-cladding chemical interaction in U-Pu-Zr metallic fuels: A critical review, Nucl. Technol. 198 (2017) 231–259. doi:10.1080/00295450.2017.1323535.
[6] C. Jiang, R. Mariani, Development of a thermodynamic database for new fuel alloy design, 2017. doi:INL/EXT-17-43324.
[7] C.T. Howard, The behavior of palladium as a getter for lanthanide fission products in U-Mo-Ti-Zr fast reactor fuels, Colorado School of Mines, 2017.
[8] H. Okamoto, Mo-U (Molybdenum-Uranium), J. Phase Equilibria Diffus. (2012). doi:10.1007/s11669-012-0095-z.
[9] R.I. Sheldon, D.E. Peterson, The U-Zr (Uranium-Zirconium) system, Bull. Alloy Phase Diagrams. (1989). doi:10.1007/BF02881432.
[10] F.A. Rough, A.A. Bauer, Constitution of uranium and thorium alloys, Battelle Memorial Inst., Columbus, Ohio, 1958.
[11] R.D. Mariani, D.L. Porter, J.R. Kennedy, S.L. Hayes, V.S. Blackwood, Z.S. Jones, D.L. Olson, B. Mishra, New fuel alloys seeking optimal solidus and phase behavior for high burnup and TRU burning, IAEA, International Atomic Energy Agency (IAEA), 2015. http://www-pub.iaea.org/MTCD/Publications/PDF/SupplementaryMaterials/P1665CD/Track5_Fuels.pdf.
[12] R.D. Mariani, Dopants for high burnup in metallic nuclear fuels, 12/702,077, 2010. https://patents.justia.com/patent/20110194667.
[13] Y. Park, N. Eriksson, R. Newell, D.D. Keiser, Y.H. Sohn, Phase decomposition of γ-U (bcc) in U-10 wt% Mo fuel alloy during hot isostatic pressing of monolithic fuel plate, J. Nucl. Mater. 480 (2016) 271–280. doi:10.1016/j.jnucmat.2016.08.022.
[14] P. Da, Z. Mi, Isothermal cross sections at 600 and 750 °C of the phase diagram of the system molybdenum-titanium-zirconium, Inorg. Mater. 3 (1967) 70–75.
[15] H. Zhang, C. Zhang, P. Zhou, Y. Du, Y. Peng, S. Liu, J. Wang, K. Li, Experimental Investigation of the Mo–Ti–Zr Ternary Phase Diagrams, J. Phase Equilibria Diffus. (2018). doi:10.1007/s11669-018-0668-6.
[16] J. Harp, L. Capriotti, F. Cappia, Postirradiation examination of recently irradiated metallic fuel concepts, (2018). https://inldigitallibrary.inl.gov/sites/sti/sti/Sort_8542.pdf.
[17] C.T. Howard, The Behavior of Palladium as A Getter for Lanthanide Fission Products in U-Mo-Ti-Zr Fast Reactor Fuels, Colorado School of Mines (2017).
[18] V.S. Blackwood, As-cast uranium-molybdenum based metallic fuel candidates and the effects of carbon addition, Colorado School of Mines (2014).
[19] V.P. Sinha, P. V. Hegde, G.J. Prasad, G.K. Dey, H.S. Kamath, Phase transformation of metastable cubic γ-phase in U-Mo alloys, J. Alloys Compd. 506 (2010) 253–262. doi:10.1016/j.jallcom.2010.06.187.
[20] N.T.H. Kim-Ngan, I. Tkach, S. Mašsková, L. Havela, A. Warren, T. Scott, Cubic γ-phase U-Mo alloys synthesized by splat-cooling, Adv. Nat. Sci. Nanosci. Nanotechnol. 4 (2013). doi:10.1088/2043-6262/4/3/035006.
[21] D.E. Janney, S.L. Hayes, Experimentally Known Properties of U-10Zr Alloys: A Critical Review, Nucl. Technol. 203 (2018) 109–128. doi:10.1080/00295450.2018.1435137.

[22] ASTM International, E407-07: Standard Practice for Microetching Metals and Alloys, ASTM Int. West Conshohocken, PA. (2012) 1–21.
[23] P. Walker, W.H. Tarn, Metal Etching Handbook, 1991.
[24] W. Zhuo, Y. Xie, M.T. Benson, Q. Yang, R.D. Mariani, J. Zhang, Experimental investigation of FCCI using diffusion couple test between UZr fuel with Sb additive and cladding, Nucl. Sci. Eng. (2020). doi:10.1080/00295639.2020.1713656.
[25] C.L. Trybus, J.E. Sanecki, S.P. Henslee, Casting of metallic fuel containing minor actinide additions, J. Nucl. Mater. 204 (1993) 50–55. doi:10.1016/0022-3115(93)90198-8.
[26] D.E. Janney, T.P.O. Holleran, Zr Inclusions in Actinide – Zr alloys : new data and ideas about how they form, J. Nucl. Mater. 460 (2015) 13–15. doi:10.1016/j.jnucmat.2015.01.065.
[27] D.E. Janney, J.R. Kennedy, J.W. Madden, T.P. O'Holleran, Crystal structure of high-Zr inclusions in an alloy containing U, Pu, Np, Am, Zr and rare-earth elements, J. Nucl. Mater. 448 (2014) 109–112. doi:10.1016/j.jnucmat.2014.01.044.
[28] S. Ahn, Comprehensive investigation of the uranium-zirconium alloy system: thermophysical properties, Phase Characterization and Ion Implantation Effects, Texas A&M University, 2013.
[29] G.L. Hofman, M.K. Meyer, S.C. Avenue, A.E. Ray, W. Lafayette, S. Paulo, Design of high density gamma-phase uranium alloys for LEU dispersion fuel applications, RERTR - Int. Meet. Reduc. Enrich. Res. Test React. (1998) 1–12.
[30] C.B. Lee, D.H. Kim, Y.H. Jung, Fission gas release and swelling model of metallic fast reactor fuel, J. Nucl. Mater. 288 (2001) 29–42. doi:10.1016/S0022-3115(00)00718-2.
[31] K.H. Kim, S.J. Oh, S.K. Kim, C.T. Lee, C.B. Lee, Microstructural characterization of U-Zr alloy fuel slugs for sodium-cooled fast reactor, in: Surf. Interface Anal., 2012. doi:10.1002/sia.4989.
[32] G. Liang, Y. Ali, G. You, M.X. Zhang, Effect of cooling rate on grain refinement of cast aluminium alloys, Materialia. (2018). doi:10.1016/j.mtla.2018.08.008.
[33] X. Guoqiang, The study of metallographic and phase structure in the U-10Zr alloy, China institute of atomic energy annual report. (1991).
[34] E.A. Nyberg, D.E. Burkes, V. V Joshi, C.A. Lavender, The Microstructure of Rolled Plates from Cast Billets of U-10Mo Alloys, Pacific Northwest Natl. Lab. (2015).
[35] D.E. Burkes, R. Prabhakaran, T. Hartmann, J.F. Jue, F.J. Rice, Properties of DU-10 wt% Mo alloys subjected to various post-rolling heat treatments, Nucl. Eng. Des. (2010). doi:10.1016/j.nucengdes.2010.02.008.
[36] W.E. Frazier, S. Hu, N. Overman, C. Lavender, V. V. Joshi, Short communication on Kinetics of grain growth and particle pinning in U-10 wt.% Mo, J. Nucl. Mater. (2018). doi:10.1016/j.jnucmat.2017.10.041.
[37] S. Jana, N. Overman, T. Varga, C. Lavender, V. V. Joshi, Phase transformation kinetics in rolled U-10 wt. % Mo foil: Effect of post-rolling heat treatment and prior γ-UMo grain size, J. Nucl. Mater. (2017). doi:10.1016/j.jnucmat.2017.09.030.